

CROSS SECTIONS FOR (n,p) REACTION ON RUTHENIUM ISOTOPES IN TERMS OF THE NOVEL MULTISTEP COMPOUND REACTION MODEL

D. KIELAN AND A. MARCINKOWSKI

Soltan Institute for Nuclear Studies
Hoża 69, 00-681 Warsaw, Poland

(Received February 14, 1994)

Cross Sections for the (n,p) reaction on $^{96,99,101,102,104}\text{Ru}$ isotopes have been adequately explained in terms of the statistical multistep direct and the novel statistical multistep compound reaction model.

PACS numbers: 25.40. Fq

1. Introduction

Recent measurements of excitation curves for the (n,p) reaction on chains of isotopes [1–4] reveal the interplay of the compound nucleus and the preequilibrium mechanisms, depending on the target neutron excess. In particular the relative importance of compound nucleus formation is reflected by the slope of the excitation curve around 14 MeV incident energy, which is descending when the compound nucleus mechanism dominates, because of the increasing competition of the (n, pn) multiparticle evaporation. On the contrary, the preequilibrium cross section increases monotonically with increasing incident energy since the multiparticle, preequilibrium emission appears to be a relatively insignificant process below 30 MeV [5].

Calculations based on the reaction model combining preequilibrium and equilibrium emissions allow a detailed study of the contributions due to the different reaction mechanisms over a broad range of incident energies and neutron excesses of the target nuclei. Of special interest is the validation of the rigorous quantum mechanical theories of preequilibrium reactions [6–8] in calculations of the isotopic cross sections. These theories distinguish two types of preequilibrium processes namely the multistep compound reactions (MSC) and the multistep direct reactions (MSD), each of different energy and angular dependence. The MSC reaction theories have been recently

modified [9] in order to allow for the gradual absorption from the entrance channel, a phenomenon accompanying MSD processes [10]. The modified theories have turned out adequate in describing the neutron emission channels [9], but they have never been used for a description of the emission of protons. It is the aim of the present paper to apply the modified theory of Feshbach, Kerman and Koonin (MFKK) for the first time to proton emission and to compare its predictions with the predictions of the original FKK theory [6], reported by Kielan *et al.* [4], as well as with experiment. Bearing in mind the results of previous analyses of neutron emission cross sections [9, 11, 12] we expect the MFKK model to yield a low proton MSC emission that becomes dominated by MSD processes in accord with angular distribution data. These expectations are to be confirmed.

In the sequel we present the theoretical formalism of MFKK (in Sec. 2). Calculations are described and the results are compared with experiment in Sec. 3. Our conclusions are gathered in Sec. 4.

2. The multistep reaction theories

Contemporary quantal theories consider the evolution of a nuclear reaction to proceed via a series of two-body collisions, forming states of increasing complexity. In each stage of the reaction a distinction is made between continuum states and quasibound states. Emissions from the continuum states result in MSD reactions and decay of the quasibound states results in MSC reactions. The compound nucleus (CN) completes the chain of the quasibound states.

2.1. The MFKK multistep compound reaction model

The modification of the original FKK theory consists only in allowing for the absorption at the successive reaction stages M . This however, reduces the MSC cross section significantly due to the rapid increase of damping of the absorbed flux towards compound nucleus at higher M . According to Marcinkowski *et al.* [9] the modified preequilibrium MSC cross section to final states at an excitation energy U is given by,

$$\frac{d\sigma}{dU} = \pi\lambda^2 \sum_{J^\pi j' S_j} \frac{2J+1}{(2I+1)(2i+1)} \sum_M 2\pi \frac{\langle \Gamma_{MJ^\pi}^j \rangle}{\langle D_{MJ^\pi} \rangle} \times \sum_{N=M}^{r-1} \sum_{\nu=N-1}^{N+1} p_N^\pi \left(\prod_{m=M}^{N-1} \frac{\langle \Gamma_{mJ}^{\downarrow} \rangle}{\langle \Gamma_{mJ} \rangle} \right) \frac{\langle \Gamma_{NJ^\pi}^{\downarrow j S_\nu} \rho_{S_\nu}^B(U) \rangle}{\langle \Gamma_{NJ} \rangle}, \quad (1)$$

where i, I, J and S are the spins of the projectile, target nucleus, composite system and the residual nucleus, respectively. The total angular momenta of

the projectile and the ejectile are j' and j . Formula (1) contains the entrance channel strength functions $2\pi\langle\Gamma\rangle/\langle D\rangle$, the factor describing the flux that survives emission prior to reaching the N -th stage (in round bracket) and the probability of emission $\langle\Gamma^\dagger\rangle/\langle\Gamma\rangle$, which occurs via the exit modes $\nu = N \pm 1, N$. The sum over M denotes summation over the gradual contributions to absorption from the incoming flux. The summation over N is bounded to preequilibrium emissions only and does not include the compound nucleus r -stage, which can be calculated according to the Hauser-Feshbach theory.

For a δ -type residual interaction the average decay width $\langle\Gamma^\dagger\rangle$ and the damping width $\langle\Gamma^\downarrow\rangle$ can be partitioned into the densities of accessible states Y multiplied by the angular momentum coupling functions X , $\langle\Gamma_N^\nu\rangle = 2\pi\vartheta^2 X_N^\nu Y_N^\nu$. The overlap integral ϑ may be evaluated by assuming that the radial wave functions of active excitons are independent of their angular momenta and are constant inside the nucleus [13]. Assuming the number of excited particles $p = N + 1$ and holes $h = N$, $p + h = n$ (excitons) one obtains practicable expressions for Y and X (see *e.g.* Refs [3, 4, 9, 11]).

The bound particle-hole level density is

$$\begin{aligned}\rho_{Sp,h}^B(U) &= \rho_{p,h}^B(U) R_n(S) \\ &= \frac{g^n}{p!h!(n-1)!} R_n(S) \sum_{k=0}^p (-1)^k \binom{p}{k} \theta(U - kB) (U - kB)^{n-1}\end{aligned}\quad (2)$$

and the spin distribution of the particle-hole states was given by Feshbach *et al.* (1980),

$$R_n(S) = \frac{(2S+1)}{2(2\pi)^{1/2}\sigma_n^3} \exp\left(-\frac{(S+\frac{1}{2})^2}{2\sigma_n^2}\right). \quad (3)$$

All throughout this paper we use the notation E , U and B for the excitation energy of the composite system, of the final nucleus and for the binding energy of the particle exciton, respectively. The factor p_N^π , which distinguishes the emission of neutrons from that of protons, was defined as the normalized probability that the nucleon risen above the Fermi level in the N -th stage is a proton. Such probabilities were given by Herman *et al.* [13].

The strength functions $2\pi\langle\Gamma_M\rangle/\langle D_M\rangle$, that describe the gradual absorption as passing from the entrance channel j' , $M = 0$, in a series of DWBA type steps via continuum, to the $(M+1)p$, Mh quasibound states involved in the successive stages M of the reaction, are calculated according

to

$$\pi\lambda^2 \sum_{J^\pi} \sum_{j'=|J-I|}^{J+I} g_J 2\pi \frac{\langle \Gamma_{MJ^\pi}^{j'} \rangle}{\langle D_{MJ^\pi} \rangle} = R_M \pi\lambda^2 \sum_{j^\pi} \sum_{j'=|J-I|}^{J+I} g_J T_{j'}. \quad (4)$$

Here g_J is the usual statistical factor of equation (1), $T_{j'}$ are the partial-wave transmission coefficients of the standard optical model and the R_M are given by the recurrence formula proposed by Marcinkowski *et al.* [9],

$$R_M = (R - R_1 - R_2 - \dots - R_{M-1}) \frac{\rho_{(M+1)p, Mh}^B}{\rho_{M+1)p, Mh}}, \quad (5)$$

with $R_0 = 0$ and $(1 - R)$ being the integrated MSD cross section expressed as a fraction of the optical model absorption cross section. The density of unrestricted states $\rho_{(M+1)p, Mh}$ was given by Ericson [14].

The double-differential MSC cross section contains only even Legendre polynomials ensuring symmetric angular distributions of the emitted nucleons.

2.2. The multistep direct reaction theory

The MSD cross section is a sum of emissions from a few subsequent collisions of the projectile inside the nucleus each creating a new particle-hole pair. Practically at incident energies lower than 20 MeV only the first step counts since the second one adds less than 5% of the onestep cross section in the investigated reactions. There are different models used in practice to calculate the onestep cross section although the existing theories derive it in a similar way [15]. According to the FKK theory the DWBA angular distributions are averaged over all allowed $1p1h$ final states of a shell model, which then contribute incoherently,

$$\frac{d^2\sigma}{dU d\Omega_{\text{onestep}}} = \sum_l (2l+1) \rho_{1,1}(U) R_2(l) \left\langle \left[\frac{d\sigma(\theta)}{d\Omega} \right]_l^{\text{DWBA}} \right\rangle. \quad (6)$$

The sum in equation (6) runs over the transferred orbital angular momenta l . The MSD cross section is sensitive to the spin cut-off parameter σ_2 in the distribution of the $1p1h$ levels $R_2(l)$ (compare Eq. (3)).

3. Calculations and comparison with experiment

The MSD cross sections consist of the onestep component calculated at the assumption that the contribution to the spins of the final states comes

only from the transferred orbital angular momentum l . For l -values from 0 to 9 the final $1p1h$ configurations have been selected according to the shell model of Seeger [16]. Only neutron(particle)-proton(hole) pairs contribute to the (n,p) reaction. The angular distributions of emitted protons that enter the average in Eq. (6) were calculated with a microscopic, two-particle form factor, for each particle-hole excitation compatible with angular momentum selection rules and with the outgoing proton energy bin, using the DWUCK-4 code [17]. A Yukawa residual interaction of 1.0 fm range and strength $V_0 = 25$ MeV was acting on the bound-state wave functions of a real Woods-Saxon potential of radius 1.2 fm and diffuseness 0.6 fm. The distorted waves for neutrons were taken from the optical potential of Wilmore and Hodgson [18] and the ones for protons from Perey [19]. Global single-particle state density $g = A/13$ was assumed and the spin cut-off parameters were evaluated from the original prescription, $\sigma_n^2 = 0.16nA^{2/3}$, given by Feshbach *et al.* [6].

In these calculations, for each 1 MeV outgoing energy bin, we have obtained about 10 microscopic angular distributions. This appeared however not enough and in order to obtain smooth proton spectra additional averaging over final $1p1h$ states contained in 5 MeV energy intervals, typical of giant resonance width, was applied.

The MSD spectra of neutrons and protons were integrated and divided by the optical model absorption cross section in order to obtain $(1 - R)$. Then R determines the fraction of the incoming flux that undergoes absorption in formulae (4) and (5). The dependence of R on projectile energy was found to be weak and therefore an average, energy independent value $R = 0.86$ has been accepted throughout the incident energy range spanned by the calculated excitation curves.

The preequilibrium MSC cross sections were calculated from formula (1). Summation over N in (1) was truncated at the $N = 4$ stage, which was estimated to contribute to only 5% of the summed MSC emission. This means that emissions from stages $N \geq 4$ were included into the compound nucleus CN cross section calculated according to the Hauser-Feshbach theory. This approach bounds also the sum over M to three terms only. The corresponding three partial entrance strength functions for passing into the $2p1h$, the $3p2h$ and the $4p3h$ quasibound states were calculated from Eqs (4) and (5) using the neutron optical potential of Ref. [18]. The ratios of the density of quasibound states to that of all states $\rho_{(M+1)p,Mh}^B(E)/\rho_{(M+1)p,Mh}(E)$, entering formula (5), appear approximately the same for ^{96}Ru , ^{99}Ru and ^{101}Ru but differ from the ones for ^{102}Ru and ^{104}Ru . The resulting R_M values are listed in Table I. The sums of $R_1 + R_2 + R_3$ from Table I do not always exhaust all the absorbed flux $R = 0.86$, which simply means that some flux gets spread, via contin-

uum, beyond the $4p3h$ quasibound states and feeds explicitly the compound nucleus.

TABLE I

R_M factors that determine the partial entrance channel strength functions according to Eqs (4) and (5).

| Incident neutron energy | Target nuclei | | | | | |
|-------------------------------|-------------------------|---------|---------|-----------------------|---------|---------|
| | $^{96,99,101}\text{Ru}$ | | | $^{102,104}\text{Ru}$ | | |
| | Reaction stage | | | Reaction stage | | |
| | $M = 1$ | $M = 2$ | $M = 3$ | $M = 1$ | $M = 2$ | $M = 3$ |
| 12 MeV | 0.33 | 0.38 | 0.15 | 0.21 | 0.32 | 0.25 |
| 14 MeV | 0.28 | 0.37 | 0.20 | 0.18 | 0.28 | 0.26 |
| 17 MeV | 0.22 | 0.33 | 0.24 | 0.13 | 0.21 | 0.25 |

The density of the bound-particle-hole levels given by formulae (2) and (3) was calculated with the same spin cut-off parameter as used in the MSD calculations. For sake of consistency we used $g = 6a/\pi^2$ when calculating the MSC cross sections. The Hauser–Feshbach compound nucleus cross sections were obtained with the level densities given by Gilbert and Cameron [20]. The parameters a were taken from the local systematics, which diversifies the features of individual isotopes [4, 21] and the spin cut-off parameter was $\sigma^2 = 0.146A^{2/3}[a(U - \Delta)]^{1/2}$. The pairing energies Δ were from Gilbert and Cameron [20].

In the MSC model only nucleon emission is allowed for, but in the Hauser–Feshbach calculations the emission of alpha particles was accounted for in addition. For protons the optical potential of Perey [19] was adopted and for alpha particles the one of McFadden and Satchler [22] was used. The radiative widths in the Hauser–Feshbach formulae were combined of single-particle and giant resonance strength functions for $E1$, $E2$ and $M1$ excitations [23].

Total reaction cross sections for the $^{96,101,104}\text{Ru}(n, p)$ reactions as well as cross sections for population of the $-1/2$ isomeric state at 143 keV and the $+5$ isomeric state at about 300 keV in the $^{99}\text{Ru}(n, p)^{99m}\text{Tc}$ and $^{102}\text{Ru}(n, p)^{102m}\text{Tc}$ reactions, respectively, have been calculated and compared with results of measurements obtained by Kielan *et al.* [4] (see Figs 1 and 2). The compound nucleus decay dominates the excitation curve for the $^{96}\text{Ru}(n, p)$ reaction but the systematic decrease of the reaction $Q_{n,p}$ value, which reaches -4.84 MeV for the ^{104}Ru target, reduces the role of proton evaporation along the isotopic chain letting the preequilibrium emission to predominate for the most neutron excessive target isotopes. The MSC cross sections calculated according to the MFKK model are lower than

those predicted by FKK (see Ref. [4]) in favour of the CN cross sections. This reduction is compensated by the increased MSD emission obtained with the FKK spin cut-off parameters $\sigma_n^2 = 0.16nA^{2/3}$ used instead of the $\sigma_n^2 = 0.28nA^{2/3}$, proposed by Reffo and Herman [24] and applied by Kielan *et al.* [4] (compare Eqs (3) and (6)).

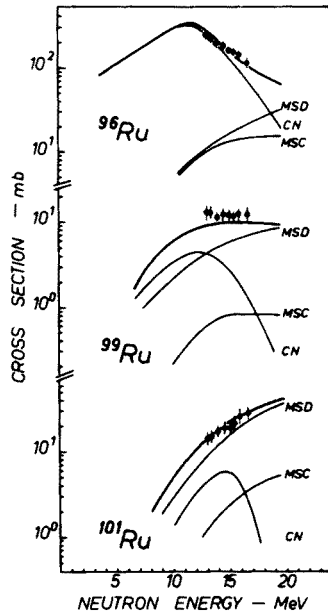


Fig. 1. Comparison of excitation curves for the $^{96,99,101}\text{Ru}(n,p)$ reactions calculated according to the MFKK model with experiment [4]. The cross sections for the $^{99}\text{Ru}(n,p)$ reaction are both experimentally and theoretically for population of the isomeric state with energy 143 keV and spin $-\frac{1}{2}$ in ^{99}Tc . The cross sections for the $^{96,101}\text{Ru}(n,p)$ reactions are total reaction cross sections. The thick solid lines represent the sums of the compound nucleus, the multistep compound and the onestep direct cross sections. The three contributions are shown separately by the thin solid lines labelled CN, MSC and MSD, respectively.

The agreement between calculations and experiment in Figs 1 and 2 is better in details than the one obtained when the FKK model was used (see Kielan *et al.* [4]), though the spin dependence of the MSD cross sections, simplified due to the assumed target spin equal 0 and projectile spin equal 0, results in the rather still low cross section for population of the low spin ($-\frac{1}{2}$) isomeric state in the $^{99}\text{Ru}(n,p)^{99m}\text{Tc}$ reaction (see Fig. 1). The choice of a better model on the basis of the calculated excitation curves is for all that difficult. Also the analysis of the proton spectrum, in Fig. 3, does not help to distinguish between the models when compared with Fig. 4

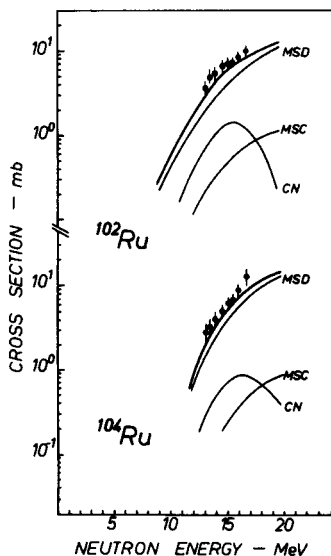


Fig. 2. The same as in Fig. 1 but for the $^{102,104}\text{Ru}(n,p)$ reactions. The cross sections for the $^{102}\text{Ru}(n,p)$ reaction are both experimentally and theoretically for the population of the isomeric state with energy about 300 keV and spin +5 in ^{102}Tc . In case of the $^{104}\text{Ru}(n,p)$ reaction total reaction cross sections are compared.

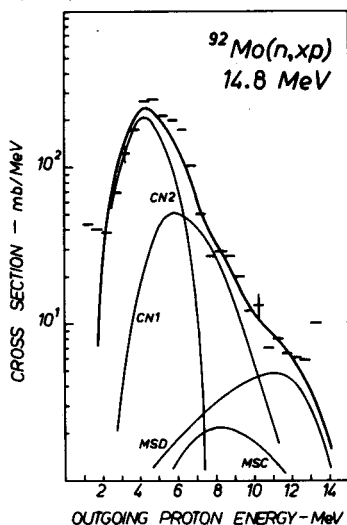


Fig. 3. The proton emission spectrum calculated according to the MFKK model compared with the result of experiment induced by 14.8 MeV neutrons on ^{92}Mo [27]. Evaporated primary CN1 and secondary CN2 (n,np) protons contribute to the compound nucleus cross section. The MSC and MSD cross sections shape the high-energy part of the spectrum. The thick solid line is the sum of the four components. This spectrum has to be compared with Fig. 4 of Kielan *et al.* [4].

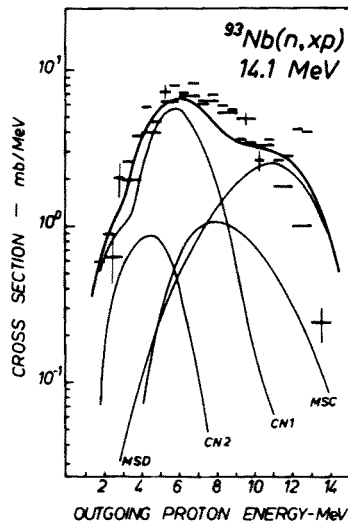


Fig. 4. The proton emission spectrum calculated according to the MFKK model compared with results of experiments induced by 14.1 MeV neutrons on ^{93}Nb . The 1 MeV bars represent the data of Traxler *et al.* [25] and the 0.5 MeV bars are from Grimes *et al.* [26]. The thick solid line is a sum of the evaporated primary CN1 and secondary CN2 (n, np) protons as well as of the preequilibrium MSC and MSD contributions.

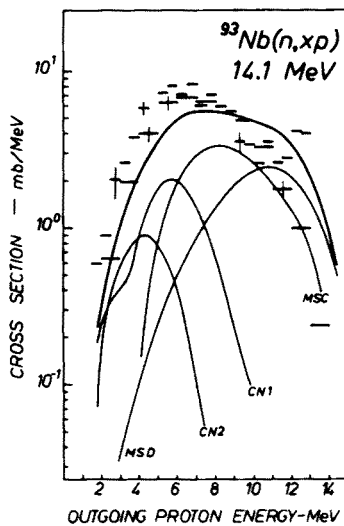


Fig. 5. The same as in Fig. 4 but calculations according to the original FKK model. The MSD cross sections remain unchanged (compare Fig. 4)

of Ref. [4]. The only resort lies thus in comparison with measured angular distributions of emitted protons. However measurements of proton angular

distributions are sparse and confined to incident neutron energies around 14 MeV. Of the few known experimental data sets we have analysed the one for the $^{93}\text{Nb}(n,p)$ reaction, which seems to be close enough to the $^{96}\text{Ru}(n,p)$ case. In Figs 4 and 5 the predictions of MFKK as well as of FKK are compared with the angle-integrated proton spectra measured by Traxler *et al.* [25] and by Grimes *et al.* [26]. One can see that only beyond 10 MeV of outgoing proton energy the two models in question differ in predicting the angular distribution. The MFKK predicts here the forward peaked MSD emission to prevail over the MSC cross sections, whereas the FKK model provides the symmetric MSC cross sections that are approximately equal to the MSD ones.

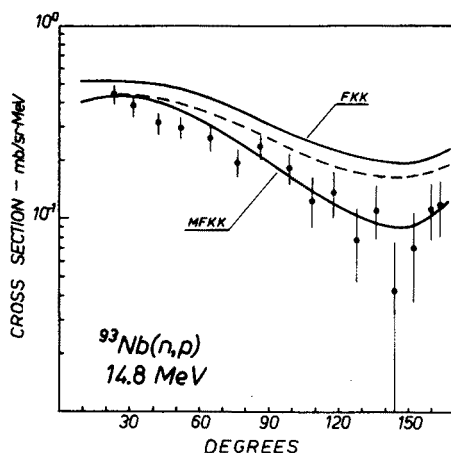


Fig. 6. Comparison of the angular distribution of protons with outgoing energies from 10 MeV to 12 MeV calculated according to the MFKK and the FKK models (as labelled) with experiment induced by 14.1 MeV neutrons on ^{93}Nb [25]. The solid lines are sums of the MSD, MSC and CN1 cross sections as given in Figs 4 and 5. The labels pertain immediately to the MSC cross sections but intermediately they pertain also to the CN1 ones, since the sum of the two is fixed due to conservation of the absorbed flux. The dashed line is the FKK result multiplied by 0.84.

In Fig. 6 the angular distribution of protons of outgoing energies between 10 MeV and 12 MeV from the $^{93}\text{Nb}(n,p)$ reaction, measured at 14.1 MeV incoming energy [25], is compared with the calculations. The MFKK double-differential MSC cross sections together with the MSD and the primary evaporation CN1 cross sections constitute the solid line labelled MFKK, which fits the experimental data well. The FKK angular distribution also after renormalization (dashed curve) reveals an excess of the symmetric MSC contribution. We thus confirm that only the MFKK model describes satisfactorily both the energy spectrum (Fig. 4) and the

angular distribution (Fig. 6) of protons emitted in the $^{93}\text{Nb}(n,p)$ reaction. This result was obtained with the spin cut-off taken from [24].

4. Conclusions

The emission of protons in neutron induced reactions is better described by the MFKK reaction model, which provides for the prevalence of direct processes in preequilibrium reactions [9, 12], though a clear distinction in favour of the MFKK model is possible above all in the case of selected, forward peaked angular distribution. This conclusion is in line with the recent observation that emission of neutrons of outgoing energies just beyond the compound nucleus domain (from about 5 MeV upwards) is forward peaked and calls positively for the MFKK [9].

REFERENCES

- [1] H.M. Hoang, U. Garuska, A. Marcinkowski, B. Zwięglinski, *Z. Phys.* **334**, 285 (1989).
- [2] H.M. Hoang, U. Garuska, D. Kielan, A. Marcinkowski, B. Zwięglinski, *Z. Phys.* **A342**, 283 (1992).
- [3] A. Marcinkowski, U. Garuska, H.M. Hoang, D. Kielan, B. Zwięglinski, *Nucl. Phys.* **A510**, 93 (1990).
- [4] D. Kielan, A. Marcinkowski, U. Garuska, *Nucl. Phys.* **A559**, 333 (1993).
- [5] M. Blann, in Proc. of Specialists Meeting on Preequilibrium Nuclear Reactions, OECD (Paris) Report NEANDC-245 "U" 1988, p.171.
- [6] H. Feshbach, A. Kerman, S. Koonin, *Ann. Phys. (N.Y.)* **125**, 429 (1980).
- [7] H. Nishioka, J.J.M. Verbaarschot, H.A. Weidenmüller, S. Yoshida, *Ann. Phys. (N.Y.)* **172**, 67 (1986).
- [8] M. Herman, G. Reffo, H.A. Weidenmüller, *Nucl. Phys.* **A356**, 124 (1992).
- [9] A. Marcinkowski, J. Rapaport, R.W. Finlay, C. Brient, M. Herman, M.B. Chadwick, *Nucl. Phys.* **A561**, 387 (1993).
- [10] H. Nishioka, H.A. Weidenmüller, S. Yoshida, *Z. Phys.* **A335**, 197 (1990).
- [11] A. Marcinkowski, J. Rapaport, R.W. Finlay, X. Aslanoglou, D. Kielan, *Nucl. Phys.* **A530**, 75 (1991).
- [12] M.B. Chadwick, P.C. Young, *Phys. Rev.* **C47**, 2255 (1993).
- [13] M. Herman, A. Marcinkowski, K. Stankiewicz, *Nucl. Phys.* **A439**, 69 (1984); *Nucl. Phys.* **A435**, 859(E) (1985).
- [14] T. Ericson, *Adv. Phys.* **9**, 425 (1960).
- [15] A. Koning, M. Akkermans, *Ann. Phys. (N.Y.)* **208**, 216 (1991).
- [16] M. Hilman, J.R. Grover, *Phys. Rev.* **185**, 1303 (1969).
- [17] P.D. Kuntz, Dept. of Physics, University of Colorado Report 1969.
- [18] D. Wilmore, P.E. Hodgson, *Nucl. Phys.* **55**, 673 (1964).
- [19] F.G. Perey, *Phys. Rev.* **131**, 745 (1963).

- [20] G. Gilbert, A.G.W. Cameron, *Can. J. Phys.* **43**, 1446 (1965).
- [21] G. Reffo, CNEN-Report, RT/FI/78, Bologna 1978.
- [22] L. McFadden, G.R. Satchler, *Nucl. Phys.* **84**, 177 (1966).
- [23] M. Herman, A. Marcinkowski, K. Stankiewicz, *Comput. Phys. Commun.* **33**, 373 (1984).
- [24] G. Reffo, M. Herman, *Lett. Nuovo Cim.* **34**, 261 (1982).
- [25] G. Traxler, A. Chalupka, R. Fischer, B. Strohmaier, M. Uhl, H. Vonach, *Nucl. Sci. Eng.* **90**, 174 (1985).
- [26] S.M. Grimes, R.C. Haight, J.D. Anderson, *Phys. Rev.* **C28**, 508 (1978).
- [27] R.C. Haight, S.M. Grimes, R.G. Johnson, H.H. Barshall, *Phys. Rev.* **C23**, 700 (1981).